

PII: S0038–1098(97)00392-X

LOW-TEMPERATURE BIREFRINGENCE IN ORDERED GaInP ALLOY STUDIED BY POLARIZED TRANSMISSION SPECTROSCOPY

Yong Zhang, B. Fluegel, A. Mascarenhas, J.F. Geisz, J.M. Olson, F. Alsina and A. Duda

National Renewable Energy Laboratory, Golden, CO 80401, U.S.A.

(Received 31 July 1997; accepted 11 August 1997 by E.E. Mendez)

The low-temperature birefringence of spontaneously ordered GaInP is studied by using polarized transmission spectroscopy at 5 K. Refractive indexes n_o , n_e and the birefringence $\Delta n_{oe} = n_o - n_e$ are obtained by applying two independent techniques: (1) measuring the polarized transmission spectra with polarization parallel to each of the two cleaved edges individually; and (2) measuring one transmission spectrum with a cross-polarization configuration. The results of these two techniques are consistent, and both give $\Delta n_{oe} \sim 0.02$ near the band-gap of partially ordered GaInP. Exact and approximate formulae have been derived for analyzing the cross-polarization spectrum. A possible device—polarization rotator—is proposed based on the in-plane birefringence. © 1997 Elsevier Science Ltd

Keywords: D. order–disorder effects, D. optical properties, A. semiconductors, C. crystal structure and symmetry.

Spontaneously generated CuPt_B ordering in the Ga_{0.5}In_{0.5}P alloy [1] changes its crystal symmetry from T_d to C_{3v} . This symmetry change results in alterations to both the electronic and optical properties of the alloys [1–3]. Because of its uniaxial symmetry, birefringence and dichroism are expected in the ordered alloy. Phenomena closely related to dichroism and birefringence have been demonstrated in ordered GaInP alloys by a variety of polarized spectroscopy methods [2, 4–9]. Not until very recently have explicit values for the *room-temperature* birefringence near the fundamental band-gap been obtained [10] by studying the light propagation in an AlGaInP/GaInP/AlGaInP waveguide. However, the technique of [10] is not only experimentally complicated, which involves making the waveguide, coupling the light into and measuring the light propagation in the waveguide, but also requires a rather sophisticated method — a transfer-matrix method for anisotropic planar waveguides — for analyzing the data. Also, the mean refractive index n was taken from another measurement in order to obtain Δn . In this work, we use two much simpler techniques, both technically and analytically, to obtain the *low-temperature* birefringence in a CuPt ordered alloy, which not only yields $\Delta n = n_o - n_e$, but also n_o and n_e (the ordinary and

extraordinary refractive indices) separately. In short, we measure the normal-incident transmission spectra with (1) polarization parallel to each of the two cleaved edges individually and (2) cross polarization between the two directions bisecting the cleaved edges. The spectra are analyzed with simple formulae which we have derived for each of the geometries. Birefringence as small as one part in a thousand can be readily measured, which was believed not to be possible by interferometric methods [10].

An 8.8 μm thick ordered GaInP epilayer with its substrate removed was used for this study. By using a relatively thick sample, the intrinsic Fabry–Perot transmission peaks become sensitive indicators of the refractive index [11]. The lattice-matched sample was grown using atmospheric-pressure organometallic vapor phase epitaxy on a (0 0 1) GaAs wafer miscut 6° toward (1 1 1)B. The sample is strongly ordered with a band gap E_g (10 K) = 1.920 eV and a valence-band splitting $E_{vbs} = 23$ meV, measured by photoluminescence excitation spectroscopy. It has large single-variant ordered domains on the order of 1 μm (measured using TEM) as well as a specular surface. The light source was a spatially filtered tungsten filament, focused to a 50 μm diameter spot. Two polarizers with extinction better than

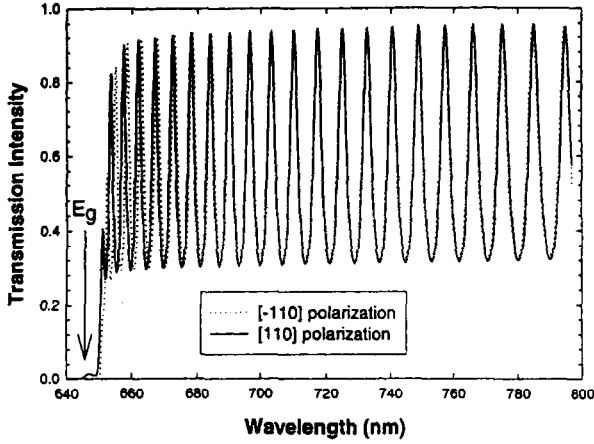


Fig. 1. Transmission spectra of an ordered GaInP₂ epilayer with the polarizations of the incident and transmitted beams both in the [1 1 0] or $[\bar{1} 1 0]$ directions.

10^{-5} were used to select the polarization of the incident and the transmitted beams.

Figure 1 shows the 5 K transmission spectra with two polarizers aligned parallel to each other either along the [1 1 0] or $[\bar{1} 1 0]$ directions (the ordering direction is defined along the [1 1 1]). The spectrum of the *e*- or [1 1 0]-polarization shifts to the short (long) wavelength side with respect to the *o*- or $[\bar{1} 1 0]$ -polarization when the wavelength λ is shorter (longer) than approximately 715 nm, which indicates the existence of the birefringence, as well as a sign change. The birefringence is clearly stronger near the bandgap and the direction of the displacement gives the sign, i.e. $n_e < n_o$ near E_g . The results of Fig. 1 are further confirmed by that of Fig. 2 which shows the transmission spectrum for cross polarization, with one polarizer aligned in the [1 0 0] direction and the other one in the orthogonal [0 1 0] direction. The increasing amplitude of the transmission for energy closer to the band-gap confirms that the birefringence is enhanced near the band gap.

where $i = o$ or θ , $\delta_i = 2\pi d n_i / \lambda$ and $r_i = (n_i - 1)/(n_i + 1)$. $c_1 = -2(r_o^2 + r_\theta^2)/[(1 - r_o^2)(1 - r_\theta^2)]$ and $c_2 = 2(1 + r_o^2 + r_\theta^2)/[(1 - r_o^2)(1 - r_\theta^2)]$. d is the sample thickness. Equation (1) has the same functional form as that for an isotropic film in air, but here the refractive indices which are different for the two polarizations are n_o and $n_\theta = n_o n_e / \sqrt{n_o^2 \sin^2(\theta - \delta\theta) + n_e^2 \cos^2(\theta - \delta\theta)}$, where $\theta = \arccos(1/\sqrt{3}) = 54.74^\circ$ is the angle between [1 1 1] and [0 0 1] directions and $\delta\theta = 6^\circ$ is the substrate tilt angle toward the [1 1 1]_B direction. Without direct access to the uniaxis, we can still obtain the refractive index along this principle axis through the relation given above.

There are a few ways of using the data of Fig. 1. Firstly, from the displacement of the extrema of interference fringes, we can obtain $\Delta n_{o\theta}/\bar{n}$ by using a relation $\Delta n_{o\theta}/\bar{n} = \Delta \lambda_{o\theta}/\bar{\lambda}$, where $\Delta n_{o\theta}$ and $\Delta \lambda_{o\theta}$ are differences, \bar{n} and $\bar{\lambda}$ are means and λ_o and λ_θ are the extremum positions for the two polarizations. This does not require knowledge of the epilayer thickness d and the exact order of the interference m , but the dispersion is assumed to be small; Secondly, if m and d are known, by applying the extremum conditions: $m\lambda = 2nd$ (maxima) or $(m + 1/2)\lambda = 2nd$ (minima) to each curve, we can obtain both n_o and n_θ . Thirdly, we can solve for n_o or n_θ by applying equation (1) to the spectra at the extrema without knowing d . However, this method requires a high accuracy in the intensity, which is much more difficult to achieve than the necessary accuracy for the extremum positions. In reality, the intensity may be affected for instances by surface scattering and the residual absorption below the band-gap. The less-than-100% transmission in Fig. 1 is likely due to surface scattering.

We can also make use of the cross polarization data of Fig. 2. Knowing d and m , we can obtain \bar{n} and $\Delta n_{o\theta}$ in the following manner. Equation (2) can be simplified as

$$T_{oe} \approx \frac{\sin^2(\delta_{o\theta}/2)(1 - \bar{r}^2)^2(1 + 2\bar{r}^2 \cos(2\bar{\delta}) + \bar{r}^4)}{[1 - 2\bar{r}^2 \cos(2\bar{\delta} - \delta_{o\theta}) + \bar{r}^4][1 - 2\bar{r}^2 \cos(2\bar{\delta} + \delta_{o\theta}) + \bar{r}^4]} \quad (3)$$

Following a general theory [12] for light propagating in a layer with optical anisotropy, assuming no absorption, we arrive at these fairly simple formulae for the transmission intensities of the three polarization configurations:

$$T_i = (1 + 4r_i^2 \sin^2(\delta_i)/(1 - r_i^2)^2)^{-1}, \quad (1)$$

$$T_{o\theta} = \frac{1}{4} \{ T_o + T_\theta - T_o T_\theta [c_1 \cos(\delta_o + \delta_\theta) + c_2 \cos(\delta_o - \delta_\theta)] \}, \quad (2)$$

where $\bar{\delta} = 2\pi d \bar{n} / \lambda$, $\delta_{o\theta} = 2\pi d \Delta n_{o\theta} / \lambda$ and $\bar{r} = (\bar{n} - 1)/(\bar{n} + 1)$. For practical purposes, equation (3) is a very good approximation even with a fairly strong anisotropy. There are two characteristic periodicities $\bar{\delta}$ and $\delta_{o\theta}$ in equation (3). $\bar{\delta}$ determines the extrema of the fine structure as shown in Fig. 2 and $\delta_{o\theta}$ describes the dephasing of the *o*- and *e*-waves and determines the extrema of the envelope of the fine structure. The extrema of the fine structure approximately appear at

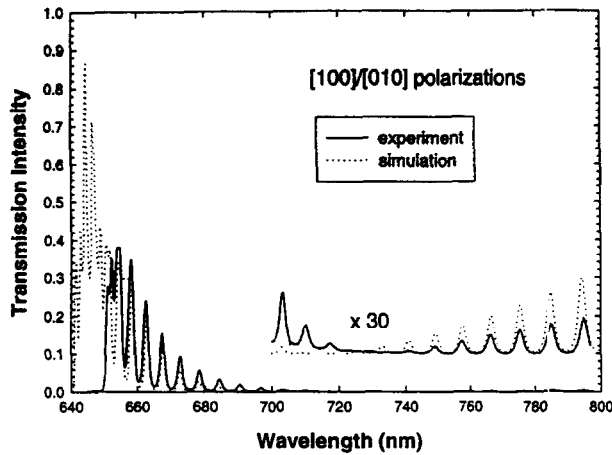


Fig. 2. Transmission spectra of an ordered GaInP₂ epilayer with the polarization of the incident beam in the [1 0 0] and that of the transmitted beam in the [0 1 0] directions.

$\lambda = 2\bar{n}d/m$ and $\lambda = 2\bar{n}d/(m + 1/2)$. The intensity at these extrema are given as

$$T_{o\theta}[\lambda = (2\bar{n}d)/m] \approx \frac{\sin^2(\delta_{o\theta}/2)(1 - \bar{r}^4)^2}{[1 - 2\bar{r}^2 \cos(\delta_{o\theta}) + \bar{r}^4]^2}, \quad (4)$$

$$T_{o\theta}[\lambda = (2\bar{n}d)/(m + 1/2)] \approx \frac{\sin^2(\delta_{o\theta}/2)(1 - \bar{r}^2)^4}{[1 + 2\bar{r}^2 \cos(\delta_{o\theta}) + \bar{r}^4]^2}. \quad (5)$$

Equations (4) and (5) are very good approximations when $\cos(\delta_{o\theta})$ is not too close to 0. When $\cos(\delta_{o\theta}) > 0$, equation (4) gives maxima and equation (5) gives minima; when $\cos(\delta_{o\theta}) < 0$, the reverse is true. According to equations (4) and (5), the envelope of the maxima or minima is mainly determined by the term $\sin^2(\delta_{o\theta}/2)$, or, when the anisotropy is very small, by $\Delta n_{o\theta}^2$.

Figure 3 shows $\Delta n_{o\theta}/\bar{n}$ by applying the first and second methods to Fig. 1. For the second method, n_o and n_θ are first obtained and then used to calculate $\Delta n_{o\theta}/\bar{n}$. The third method is used to determine the thickness d as $8.8 \pm 0.1 \mu\text{m}$, which agrees with the measured value using profilometry to within $0.2 \mu\text{m}$. The orders of the interference fringes are determined by comparing the extrema at two sample positions with thickness differing by one half wavelength and the value $m_0 = 69$ is identified for the first maximum. Also shown in Fig. 3 is $\Delta n_{o\theta}/\bar{n}$ obtained by analyzing the cross-polarization data, where the \bar{n} are calculated at the extrema and $\Delta n_{o\theta}$ are obtained by solving equation (4), with its sign assigned according to the direction of the displacement shown in Fig. 1. The results of these three different methods are reasonably close to each other. The first method is expected to exhibit a systematic error in

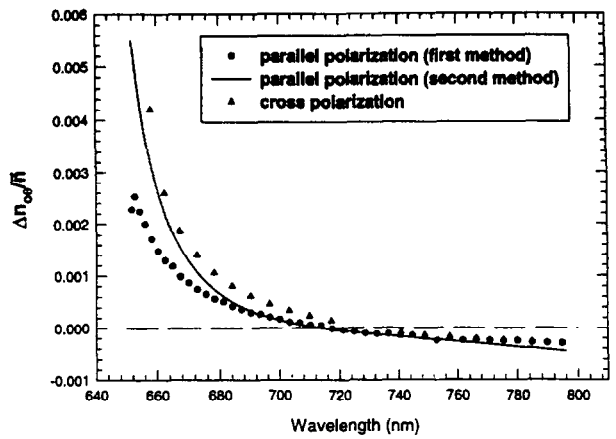


Fig. 3. Relative difference of n_o and n_θ obtained by three different methods of analyzing the polarized transmission spectra.

the region where the dispersion is not so small, as seen near the band-gap.

To check the consistency of our analysis, we generate the cross-polarization curve with n_o and n_θ obtained from the parallel-polarization data, as plotted in Fig. 2. The simulated curve is indeed very close to the real experimental result. The deviation near the band-gap is because the absorption is not considered in the simulation. As shown in the simulated curve, nearly 100% transmission, i.e. a 90° rotation of the polarization, is realized near the band-gap when the absorption is ignored. In fact, it is possible to shift the appearance of the 90°-rotation to a wavelength further away from the band-gap by increasing the epilayer thickness or the degree of ordering, which may lead to a possible device application of this feature in for example a polarization rotator.

Finally, the birefringence $n_o - n_e$ obtained from the parallel and cross polarization data are shown in Fig. 4. Although the magnitude of the birefringence obtained in this work is similar to that of [10] (because of the similar band-gap reductions), low-temperature data will be more useful for comparing with future theoretical calculation, since at room temperature, the birefringence near the band gap is distorted by the broadened absorption spectrum.

It is worth pointing out that the cross-polarization technique has been used previously to study the birefringence in semiconductor quantum wells [13–15], where the birefringence is obtained by analyzing the undulation of the envelope describing by $\sin^2(\delta_{o\theta}/2)$ [15] or the extrema determined by the dephasing $\delta_{o\theta}$ [13, 14]. For a more accurate analysis, equations (2)–(5) should be used.

The birefringence is related to the ordering induced change in the band structure. The sign of the birefringence can be understood as a result of the polarization

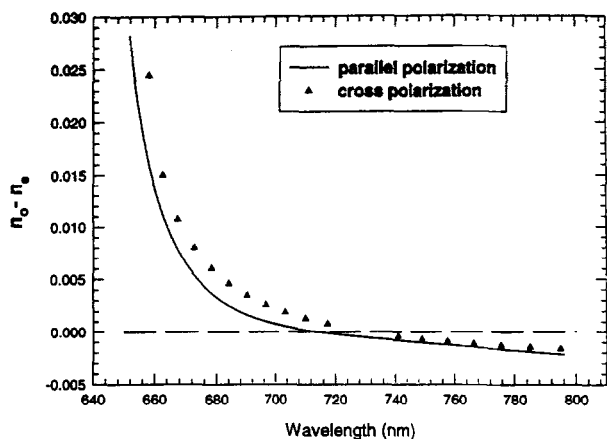


Fig. 4. Birefringence obtained by analyzing parallel and cross polarization transmission spectra.

dependence of the transition matrix element, because the contribution of each individual band to the dielectric constant is proportional to the square of the matrix element. As the topmost valence-band states in an ordered alloy have the symmetry $[3/2, \pm 3/2]_{[111]}$, the transition matrix element is much smaller for the $[111]$ polarization than for the $[\bar{1}10]$ [16]. This is the key factor which determines that $n_o > n_e$ near the band-gap, although the quantitative difference includes the contribution from other bands. The line-shape of the dielectric function near the band gap has been modeled by an eight-band $\mathbf{k}\cdot\mathbf{p}$ model in a study of reflectance difference spectroscopy of the ordered GaInP [17]. From that study, the birefringence is expected to maximize at the band-gap and changes sign above the band-gap.

In summary, for first time the low-temperature birefringence of ordered GaInP has been obtained by applying two techniques of polarized transmission spectroscopy: (1) two parallel polarizations and (2) one cross-polarization. The first technique is similar to that used to measure the average refractive index in [11]. The second is intuitively similar to ellipsometry, but much more immune to surface artifacts. The spectra reveal the birefringence in a straightforward and transparent way and the quantitative analysis is relatively simple using the formulae derived. The measurement and the analysis are for crystals with trigonal symmetry, but they are applicable to crystals with other uniaxial symmetry. The results of the two methods are consistent and both give $\Delta n \sim 0.02$ near the band-gap of partially ordered GaInP.

Acknowledgements—This work was supported by the Office of Energy Research, Material Science Division of DOE under contract No. DE-AC36-83CH10093.

REFERENCES

- Gomyo, A., Suzuki, T. and Iijima, S., *Phys. Rev. Lett.*, **60**, 1988, 2645.
- Mascarenhas, A., Kurtz, S., Kibbler, A. and Olson, J.M., *Phys. Rev. Lett.*, **63**, 1989, 2108.
- Ernst, P., Zhang, Yong, Driessen, F.A.J.M., Geng, C., Jones, E.D., Mascarenhas, A., Scholz, F. and Schweizer, H., *J. Appl. Phys.*, **81**, 1997, 2814.
- Horner, G.S., Mascarenhas, A., Alonso, R.G., Friedman, D.J., Sinha, K., Bertness, K.A., Zhu, J.G. and Olson, J.M., *Phys. Rev.*, **B48**, 1993, 4944.
- Kita, T., Fujiwara, A., Nakayama, H. and Nishino, T., *Appl. Phys. Lett.*, **66**, 1995, 1794.
- Alsina, F., Garriga, M., Alonso, M.I., Pascual, J., Camassel, J. and Glew, R.W., in *Physics of Semiconductors—Proc. 22nd Int. Conf. Vancouver, Canada, 1994* (Edited by D.J. Lockwood), p. 253. World Scientific, Singapore, 1995).
- Schubert, M., Rheinlander, B. and Gottschalch, V., *Solid State Commun.*, **95**, 1995, 723.
- Luo, S., Olson, J.M., Bertness, K.A., Raikh, M.E. and Tsiper, E.V., *J. Vac. Sci. Technol.*, **B12**, 1994, 2552.
- Moritz, A., Wirth, R., Geng, C., Scholz, F. and Hangleiter, A., *Mat. Res. Soc. Symp. Proc.*, **417**, 1995, 97.
- Wirth, R., Moritz, A., Geng, C., Scholz, F. and Hangleiter, A., *Phys. Rev.*, **B55**, 1997, 1730.
- Moser, M., Winterhoff, R., Geng, C., Queisser, I., Scholz, F. and Dornen, A., *Appl. Phys. Lett.*, **64**, 1994, 235.
- Yeh, P., *Surf. Sci.*, **96**, 1980, 41.
- Pamulapati, J., Loehr, J.P., Singh, J. and Bhattacharya, P.K., *J. Appl. Phys.*, **69**, 1991, 4071.
- Fainstein, A., Etchegoin, P., Santos, P.V., Cardona, M. and Totemeyer, K., *Phys. Rev.*, **B50**, 1994, 11850.
- Etchegoin, P., Fainstein, A., Sirenko, A.A., Koopmans, B., Richards, B., Santos, P.V., Cardona, M., Totemeyer, K. and Eberl, K., *Phys. Rev.*, **B53**, 1996, 13662.
- Zhang, Yong, Mascarenhas, A., Ernst, P., Driessen, F.A.J.M., Friedman, D.J., Bertness, K.A., Olson, J.M., Geng, C., Scholz, F. and Schweizer, H., *J. Appl. Phys.*, **81**, 1997, 6365.
- Luo, J.S., Olson, J.M., Zhang, Yong and Mascarenhas, A., *Phys. Rev.*, **B55**, 1997, 16385.